

Using bond-length dependent transferable force constants to predict vibrational entropies in Au-Cu, Au-Pd, and Cu-Pd alloys

Eric J. Wu and Gerbrand Ceder

*Department of Materials Science and Engineering,
Massachusetts Institute of Technology, Cambridge, MA 02139, USA*

Axel van de Walle

*Department of Materials Science and Engineering,
Northwestern University, Evanston, IL 60208, USA*

A model is tested to rapidly evaluate the vibrational properties of alloys with site disorder. It is shown that length-dependent transferable force constants exist, and can be used to accurately predict the vibrational entropy of substitutionally ordered and disordered structures in Au-Cu, Au-Pd, and Cu-Pd. For each relevant force constant, a length-dependent function is determined and fitted to force constants obtained from first-principles pseudopotential calculations. We show that these transferable force constants can accurately predict vibrational entropies of L1₂-ordered and disordered phases in Cu₃Au, Au₃Pd, Pd₃Au, Cu₃Pd, and Pd₃Au. In addition, we calculate the vibrational entropy difference between L1₂-ordered and disordered phases of Au₃Cu and Cu₃Pt.

I. INTRODUCTION

In the last decade, a clear prescription has emerged to obtain phase diagrams of materials from first-principles. When two compounds mix, some amount of site disorder occurs. First-principles alloy theory has been mostly preoccupied with defining appropriate energy models for such partially disordered systems, and obtaining the parameters for them from increasingly accurate Density Function Theory (DFT) methods. In particular, the cluster expansion approach¹ has been highly successful, as it allows one to parameterize the energy of systems with disorder on a fixed framework of sites. Many binary phase diagrams have been calculated in this way²⁻⁶.

Most of these first-principles phase diagram calculations do not include vibrational entropy effects. The assumption that vibrational entropy differences between phases are small, and can therefore be neglected, has been recently examined experimentally⁷⁻¹¹ and theoretically¹²⁻¹⁸. In Al₂Cu¹⁸ vibrational entropy contributions were shown to be essential in reversing the stability of θ and θ' phases at finite temperatures. In the Al-Sc system, vibrational entropy contributions were shown to increase the solubility limits 27-fold^{16,17}.

For alloys with partial site disorder, vibrational entropy in first-principles phase diagrams is computationally intensive to determine. In conventional first-principles alloy theory, a cluster expansion has to be fit to the ground state energies of a large number of A-B ordered states (for a binary alloy). Vibrational effects can be formally included by fitting to vibrational free energies, rather than ground state energies¹⁹. This requires that one determines the phonon spectrum for many configurations. Unfortunately, this is computationally expensive.

One idea that has been proposed to alleviate this problem is the use of force constants that can be transferred between different environments. The existence of transferable force constants would greatly reduce the number of calculations required to determine vibrational entropies from first-principles: currently, almost all of the work in calculating vibrational entropies is involved with the numerical determination of force constants for every environment in a large number of structures.

The idea of using transferable force constants to reduce computational expense is tremendously appealing. Despite this, until recently, there was little clear evidence supporting the validity of their use. For instance, experimental data in Fe₃Al shows that force constants can have a clear configurational dependence²⁰. Strictly speaking, it is not possible to rigorously define configuration-independent force constant matrices as the form of the force constant matrix depends on the symmetry of the configuration²¹. Nevertheless, configuration-independent transferable force constants have been used in computations to study segregation in Ni₃Al²² and elastic properties in Li-Al²³. In Li-Al, these force constants predicted elastic constants well, but reproduced vibrational entropies poorly. Transferable force constants have also been explored in oxides²⁴ and semiconductors²⁵. In these materials, transferability is examined in the short-ranged force constants, which are obtained after subtracting out an analytical long-ranged dipole-dipole contribution. None of these studies examined the use of transferable force constants to calculate vibrational entropy. This is a challenging issue, as vibrational entropy differences between structures are a fraction of the total vibrational entropy and hence, high relative accuracy is required.

Previous attempts at defining transferable force constant matrices²³ defined force constant matrices for a given pair type. Recently, it was shown that high-accuracy in predicting the vibrational entropy could be achieved by using bond length-dependent transferable force constants^{12,26}. This simple bond length-dependent force constant model

was shown to work well in predicting vibrational entropies in Ni_3Al and Pd_3V ^{12,13}. The force constants were found to be transferable between different FCC structures at a single composition; their transferability between configurations with different atomic ratios or different chemical systems was untested.

In this paper, we evaluate the accuracy of the length-dependent transferable force constants approach in calculating vibrational entropies in the Au-Cu, Au-Pd, and Cu-Pd systems, and also investigate the transferability of such relations *between* different chemical systems. Our results show that in the Au-Cu, Au-Pd, and Cu-Pd systems, transferable force constants can be defined that depend on length and pair type. We show that these force constants can be exchanged between different structures and chemical systems, while still retaining good accuracy for calculating the vibrational entropy of intermetallic structures.

II. METHODOLOGY

A supercell method was used to calculate force constants^{12,26-29}. This method consists of creating a series of supercells with well-chosen displacements, calculating the resulting forces on atoms, then using a least-squares fit to obtain the force constants. All total energy and force calculations were performed using the Vienna *ab initio* Simulation Package (VASP)^{30,31}, which implements Blöchl's projector augmented wave (PAW) approach^{32,33} within the local density approximation (LDA). The calculations used energy cutoffs of 300-400 eV and \sim 150-200 unique \vec{k} -points per 4 atoms. This resulted in energies converged to \sim 5 meV, and forces converged to 1%. Special care was taken to make sure forces on the initial structure vanished before supercell configurations were generated for the force constant calculation.

The superstructures and their perturbations were determined using an efficient algorithm²⁶, which generates supercells with perturbed atoms and their corresponding set of linear equations. Third-order anharmonic terms, which are present when positive and negative displacements are not symmetrically equivalent, were eliminated by subtracting forces taken from calculations of perturbations of equal magnitude but opposite sign²⁶. Vibrational entropy calculations were converged to within $0.015 k_B$: this value is obtained by calculating the configuration-dependent part of the high-temperature limit of the vibrational entropy per atom, $S_{vib} = -k_B \int_0^\infty g(\omega) \ln \omega d\omega$, for increasing force constant range until S_{vib} changed by less than $0.015 k_B$. Typically, this requires \sim 4-5 neighbors for L1_2 structures and 2 neighbors for SQS-8 structures.

The above procedure was applied to calculate vibrational entropies of L1_2 -ordered and disordered phases in the Au_3Cu , Cu_3Au , Au_3Pd , Pd_3Au , Cu_3Pd , Pd_3Au , and Cu_3Pt systems. In addition, we calculated vibrational entropies of L1_2 -ordered Ag_3Au and Au_3Ag . The disordered structure was approximated by an 8 atom special quasirandom structure (SQS)³⁴. These structures have been shown to give the best possible approximation to a disordered structure, within a given number of sites. In Ni_3Al , Morgan et. al. tested the convergence of vibrational properties with SQS size, and found that a SQS with 8 atoms is a good approximation of the disordered state³⁵. The SQS-8 used in this study has been used successfully in first-principles vibrational entropy calculations of disordered Ni_3Al and Pd_3V ^{12,13}.

To define transferable force constant matrices, some approximations are necessary. The form of a force constant matrix, and hence the number of non-zero force constants, depends on the symmetry of structure. In this work, we use a stretching-bending force constant model. In this model, the coordinate system of each force constant matrix is transformed, so that the z -axis is aligned along the segment joining the two atoms in question. Two further approximations are necessary to obtain transferable force constants. First, bending terms are averaged, so that they are orientation independent. Second, off-diagonal terms are constrained to be zero. The resulting force constant matrix has only two independent terms - a stretching term s , and a bending term b - and the form of the matrix can be written

$$\begin{pmatrix} b & 0 & 0 \\ 0 & b & 0 \\ 0 & 0 & s \end{pmatrix} . \quad (1)$$

The stretching term (s) can be used as a qualitative measure of the bond strength. However, it is not possible to keep only the stretching terms (s) in the force constant matrix: doing so can result in large errors ($0.2 k_B$) in the vibrational entropy^{12,26}. We examined two types of errors associated with using stretching-bending force constant matrices: errors introduced in the force constants and errors introduced in the vibrational entropy. For all force constant matrices examined, the rms error associated with constraining the bending terms to be equal was 0.052 eV/ Å^2 per bending term. The rms error associated with setting off-diagonal terms to zero was 0.009 eV/ Å^2 per

off-diagonal term. Stretching terms contain no errors associated with the stretching-bending force constant model: they are directly obtained from the coordinate transformation, with no further approximations.

The errors introduced into the vibrational entropy by using the stretching-bending force constant model are shown in Table 1. For 14 out of the 16 structures tested, S_{vib} calculated using full-force constant matrices and S_{vib} calculated using the stretching-bending force constant model agreed to within $0.01 k_B$. For the L1₂ Au₃Cu structure, the stretching-bending force constant approximation failed when using nearest-neighbor force constants; for the SQS-8 Au₃Cu structure, the stretching-bending force constant approximation failed when using both nearest-neighbor and all-neighbor force constants (where “all-neighbor” is defined as the force constant range at which vibrational entropies were converged to within $0.015 k_B$). In these structures, using stretching-bending force constant matrices resulted in a dynamically unstable structure. Tests of each approximation revealed that the negative phonon modes in the L1₂ Au₃Cu structure arise because the off-diagonal terms set to zero; negative phonon modes in the SQS-8 Au₃Cu arise due to both the neglect of the off-diagonal terms and the constraint on the bending terms. In previous work, the errors in vibrational entropy by using the simplified stretching-bending force constant model have been tested for five structures in the Ni₃Al and Pd₃V system^{12,13}. In those systems, the errors on vibrational entropy for all structures were less than $0.01 k_B/\text{atom}$.

III. RESULTS AND DISCUSSION

Calculated vibrational entropies for all structures examined in the Ag-Ag, Au-Cu, Au-Pd, Cu-Pt, and Cu-Pd system are listed in Table 1. For the Cu-Au system, our results can be compared with previous experimental^{10,36} and theoretical¹⁴ work. We calculated $S_{vib}(Cu) = 4.87 k_B$ and $S_{vib}(Au) = 2.85 k_B$, which yields for the formation entropies $S_{vib}^{form}(L1_2 Cu_3Au) = 0.10 k_B$ and $S_{vib}^{form}(L1_2 Au_3Cu) = 0.11 k_B$. Our calculated $S_{vib}^{form}(L1_2 Cu_3Au)$ agrees well with previous experimental work, which found $S_{vib}^{form}(L1_2 Cu_3Au) = 0.07 \pm 0.03 k_B$ ³⁶. Our calculated formation entropies also agree well with previous theoretical work, which found $S_{vib}^{form}(L1_2 Cu_3Au) = 0.10 k_B$ and $S_{vib}^{form}(L1_2 Au_3Cu) = 0.14 k_B$ ¹⁴. The entropy change upon disordering in Cu₃Au ($\Delta S_{vib}^{order \rightarrow disorder}(Cu_3Au)$) is calculated to be $0.07 \pm 0.045 k_B$. This value is lower than the experimental value of $0.14 \pm 0.05 k_B$ ¹⁰. However, this calculation is in good agreement with previous theoretical work, in which $\Delta S_{vib}^{order \rightarrow disorder}(Cu_3Au) = 0.08 k_B$ was obtained¹⁴. For Au₃Cu, we calculate $\Delta S_{vib}^{order \rightarrow disorder}(Au_3Cu) = -0.01 \pm 0.03 k_B$, which is lower than the previously calculated $\Delta S_{vib}^{order \rightarrow disorder}(Au_3Cu) = 0.05 k_B$ ¹⁴.

Calculated full force constant matrices were transformed to the stretching-bending force constant model, with the results plotted in Figures 1-6. The different bond lengths correspond to equilibrium bond lengths in various structures. For all pair types, the force constant stiffness for both stretching and bending terms decreases with increasing bond length. In particular, the stiffness of first nearest-neighbor force-constant matrices shows a strong dependence on bond length. This dependence of bond stiffness on bond length shows that one can not rely too much upon simple bond-counting arguments²⁶ when predicting or explaining vibrational entropy differences between phases because the bond counting effect does not take into account bond-length changes upon disordering. Figures 1-6 show that small changes in bond length upon disordering can have a large effect on force constants and vibrational entropy. The relationship between atomic relaxations and vibrational entropy has been previously noted^{12,16-18}.

For a given bond type, stretching and bending force constants for all systems and structures are found to lie on a single curve. Thus, the dependence of bond stiffness on ordering, composition, or chemical system can be explained almost entirely in terms of bond length changes. Remarkably, other effects on force constant stiffness, such as changes in charge density associated with different configurations and chemical systems, are small. This may be because our study is limited to noble-metal intermetallics.

For each pair type, we constructed a relationship between force constant stiffness and bond length. Our goal is to parameterize the stiffness of the stretching and bending force constants as a function of bond length, then use “fitted” force constants from these functions to predict vibrational entropy. Stretching terms were fit to a second-order polynomial; bending terms were fit to a linear function. The fit was restricted to first-nearest neighbors force constants. The rms fitting error over all stretching terms was $0.102 \text{ eV}/\text{A}^2$; the rms fitting error over all bending terms was $0.048 \text{ eV}/\text{A}^2$.

Although attempts to use longer-ranged fitted force constants were unsuccessful, the errors introduced by using only nearest-neighbor force constants was small. In the systems studied, vibrational entropy converged quickly with respect to neighbors: the difference between S_{vib} calculated using only first nearest-neighbors and S_{vib} calculated using all neighbors was typically around $\sim 0.00-0.02 k_B$, with a maximum difference of $0.03 k_B$ in L1₂ Pd₃Cu. Previous studies on intermetallics and group-IV semiconductors have also shown that vibrational entropy can converge quickly with respect to neighbors^{12,13,37}.

The results of using fitted force constants to predict vibrational entropies are shown in Table 1. For all structures,

the vibrational entropies obtained using fitted force constants agree well with the vibrational entropies obtained using directly calculated force constants. The rms error between $S_{vib}^{calc, all\ neigh, full\ fc}$, and $S_{vib}^{fit, 1nn, sb}$ for all structures investigated was $0.032\ k_B$, with a maximum error of $0.058\ k_B$ in $L1_2\ Pd_3Au$. The errors are $\sim 1\text{-}2\%$ of the absolute vibrational entropy. These calculations show the predictive power of using fitted stretching-bending force constants to predict vibrational entropies.

We also tested the accuracy of using fitted force constants, in representing the effect of homogeneous volume changes. In metals, pairwise expansion can usually not capture the effect of such electron density changes of the energy. The force constants and vibrational entropy of $L1_2$ and SQS-8 structures for Pd_3Cu , Pd_3Au , Cu_3Pd , Cu_3Au , and Au_3Pd were recalculated at a volume $\sim 2\%$ larger than the equilibrium volume. For the $L1_2\ Pd_3Cu$ structure, the vibrational entropies were also calculated at a 4% and 6% volume increase were also calculated. These direct results were then compared with predicted results obtained from using force constants derived from equilibrium volume calculations. None of the force constants at these increased volumes were included in the fit. The results of using these fitted force constants to predict vibrational entropy are shown in Table 2. For all structures at 2% increased volume, the rms error between $S_{vib}^{calc, all\ neigh, full\ fc}$ and $S_{vib}^{fit, 1nn, sb}$ was $0.033\ k_B$, with a maximum error of $0.053\ k_B$ in $L1_2\ Pd_3Au$. Thus, even when the force constant data is not included in the fit, the length dependent force constant function gives force constants that accurately predict vibrational entropies.

Often, one is interested in vibrational entropy differences, rather than absolute vibrational entropies. We used vibrational entropy data from Tables 1-2 to obtain two types of vibrational entropy differences that are of interest: the vibrational entropy difference between ordered and disordered phases, and vibrational entropy difference between a structure at two volumes separated by $\sim 2\%$. The latter is related to the thermal expansion by the expression $\alpha_L = \frac{\Delta S}{3B\Delta V}$, where B is the bulk modulus. This data is shown in Table 3. In the systems studied, we estimated the effect of vibrations on calculated phase boundaries by using the following procedure: The change in transition temperature

when vibrations are included in the phase diagram calculation is given by $T_{config+vib}^{\alpha \rightarrow \beta} = T_{config\ only}^{\alpha \rightarrow \beta} \left(1 + \frac{\Delta S_{vib}^{\alpha \rightarrow \beta}}{\Delta S_{config}^{\alpha \rightarrow \beta}}\right)^{14}$.

Thus, $\frac{\Delta S_{vib}^{\alpha \rightarrow \beta}}{\Delta S_{config}^{\alpha \rightarrow \beta}}$ determines the effect of lattice vibrations on calculated phase diagrams. The configurational entropy per atom for a binary solid solution depends on the state of short-range order. It has a maximum value for an ideal (random) solution of $S_{config}^{\alpha} = k[c \ln c + (1-c) \ln(1-c)]$. Hence, the maximum value of $\Delta S_{config}^{\alpha \rightarrow \beta}$ in the systems studied is $0.562\ k_B$ /atom: this value occurs when a fully ordered state ($S_{config}^{\alpha} = 0$) at $c = 0.25$ transforms to a fully random solid solution. In most cases, the actual value of $\Delta S_{config}^{\alpha \rightarrow \beta}$ will be smaller than this, owing to short-range order in the disordered state and also some disorder in the low temperature phase. Nevertheless, our approximate estimate shows that phase boundaries in the systems studied would change by $\sim 5\text{-}13\%$ if vibrations were included.

The data in Table 3 can be used to examine the ability of transferable force constants to predict vibrational entropy differences. The rms error between calculated and fit differences $(\Delta S_{vib}^{calc, all\ neigh, full\ fc} - \Delta S_{vib}^{fit, 1nn, sb})$ was $0.030\ k_B$, with a maximum error of $0.063\ k_B$ in Cu_3Au . For vibrational entropy differences between structures at volumes 2% apart, the rms error between calculated and fit differences was $0.016\ k_B$ with a maximum error of $0.030\ k_B$ in $L1_2\ Au_3Pd$. Thus, the transferable force constants used here are able to predict vibrational entropy differences reasonably well.

In examining the data, one can make a few observations with respect to the accuracy of using transferable force constants. First, errors in absolute entropies from using transferable force constants (Tables 1-2) were typically $\sim 0.00\text{-}0.05\ k_B$ for all structures. This was true for structures with both large and small absolute vibrational entropies. Second, in all cases, the transferable force constants were able to correctly predict the relative hierarchy of entropy differences. Thus, large entropy differences are predicted to be large; small entropy differences are predicted to be small. A small entropy difference was never predicted to be large, or vice versa. Third, when using transferable force constants, errors in entropy differences between the same structure at different volumes tended to cancel; errors in entropy differences between different structures (at the same composition) did not tend to cancel as much (Table 3). Thus, it is likely that there are small structure-dependent contributions to the force constant stiffness that are not captured by our length-dependence force constant model. Fourth, using transferable force constants gave small absolute errors on vibrational entropy differences ($\sim 0.00\text{-}0.07\ k_B$). For small vibrational entropy differences, this sometimes resulted in $\sim 15\text{-}20\%$ errors, whereas the percentage errors in larger vibrational entropy differences were smaller. Lastly, this method can greatly reduce the computational cost of calculating vibrational properties of intermetallics.

IV. CONCLUSION

The vibrational entropies for 16 structures in the Ag-Au, Au-Cu, Au-Pd, Cu-Pd, and Cu-Pt systems have been calculated. A simplified model was used with only stretching and bending terms, making the force constant matrices

independent of symmetry. With these approximations, the form of the force constant matrices was independent of crystal symmetry. We found that the variation of force constants with ordering, composition, or chemical system can be explained almost entirely through changes in bond length. This method represents a promising way to include vibrational effects in phase diagram calculations at a moderate computational cost.

Acknowledgements

This work was supported by Department of Energy, Office of Basic Energy Sciences under Contract No. DE-FG02-96ER45571. We gratefully acknowledge computing resources provided by NPACI through the Texas Advanced Computing Center. We would also like to thank postdoctoral researcher Dane Morgan for insightful observations.

- ¹J. M. Sanchez, F. Ducastelle, and D. Gratias, *Physica A*, **128a**, 334 (1984).
- ²F. Ducastelle, *Order and phase stability in alloys*, Elsevier Science Pub. Co., Amsterdam, 1991.
- ³D. de Fontaine, *Solid State Physics*, **47**, 33 (1994).
- ⁴G. Ceder, M. Asta, and D. de Fontaine, *Physica C*, **177**, 106 (1991).
- ⁵A. Zunger, in *NATO ASI on Statics and Dynamics of Alloy Phase Transformations*, edited by P. E. Turchi and A. Gonis Plenum Press, New York, 1994, Vol. p.361.
- ⁶M. Asta, R. McCormack, and D. de Fontaine, *Phys. Rev. B*, **48**, 748 (1993).
- ⁷B. Fultz, L. Anthony, L. J. Nagel, et al., *Phys. Rev. B*, **52**, 3315 (1995).
- ⁸L. Anthony, J. K. Okamoto, and B. Fultz, *Phys. Rev. Lett.*, **70**, 1128 (1993).
- ⁹L. Anthony, L. J. Nagel, J. K. Okamoto, et al., *Phys. Rev. Lett.*, **73**, 3034 (1994).
- ¹⁰L. J. Nagel, L. Anthony, and B. Fultz, *Philos. Mag. Lett.*, **72**, 421 (1995).
- ¹¹M. E. Manley and B. Fultz, *Philos. Mag. B*, **80**, 1167 (2000).
- ¹²A. van de Walle and G. Ceder, *Phys. Rev. B*, **61**, 5972 (2000).
- ¹³A. van de Walle, G. Ceder, and U. V. Waghmare, *Phys. Rev. Lett.*, **80**, 4911 (1998).
- ¹⁴V. Ozolins, C. Wolverton, and A. Zunger, *Phys. Rev. B*, **58**, R5897 (1998).
- ¹⁵P. D. Tepesch, A. F. Kohan, G. D. Garbulsky, et al., *J. Am. Ceram. Soc.*, **79**, 2033 (1996).
- ¹⁶V. Ozolins and M. Asta, *Phys. Rev. Lett.*, **86**, 448 (2001).
- ¹⁷M. Asta and V. Ozolins, *Phys. Rev. B*, **64**, art. no. 094104 (2001).
- ¹⁸C. Wolverton and V. Ozolins, *Phys. Rev. Lett.*, **86**, 5518 (2001).
- ¹⁹G. D. Garbulsky and G. Ceder, *Phys. Rev. B*, **49**, 6327 (1994).
- ²⁰I. M. Robertson, *J. Phys.: Condens. Matter*, **3**, 8181 (1991).
- ²¹M. Sluiter, M. Weinert, and Y. Kawazoe, *Europhys. Lett.*, **43**, 183 (1998).
- ²²M. Sluiter and Y. Kawazoe, *Philos. Mag. A*, **78**, 1353 (1998).
- ²³M. H. F. Sluiter, M. Weinert, and Y. Kawazoe, *Phys. Rev. B*, **59**, 4100 (1999).
- ²⁴P. Ghosez, E. Cockayne, U. V. Waghmare, et al., *Phys. Rev. B*, **60**, 836 (1999).
- ²⁵P. Giannozzi, S. de Gironcoli, P. Pavone, et al., *Phys. Rev. B*, **43**, 7231 (1991).
- ²⁶A. van de Walle and G. Ceder, *Rev. Modern Phys.*, **74**, 11 (2002).
- ²⁷S. Wei and M. Y. Chou, *Phys. Rev. Lett.*, **69**, 2799 (1992).
- ²⁸S. Wei and M. Y. Chou, *Phys. Rev. B*, **50**, 2221 (1994).
- ²⁹K. Kunc and R. M. Martin, *Phys. Rev. Lett.*, **48**, 406 (1982).
- ³⁰G. Kresse and J. Furthmuller, *Comp. Mater. Sci.*, **6**, 15 (1996).
- ³¹G. Kresse and J. Furthmuller, *Phys. Rev. B*, **54**, 11169 (1996).
- ³²G. Kresse and D. Joubert, *Phys. Rev. B*, **59**, 1758 (1999).
- ³³P. E. Blochl, *Phys. Rev. B*, **50**, 17953 (1994).
- ³⁴A. Zunger, S. H. Wei, L. G. Ferreira, et al., *Phys. Rev. Lett.*, **65**, 353 (1990).
- ³⁵D. Morgan, J. D. Althoff, and D. de Fontaine, *J. Phase Equilib.*, **19**, 559 (1998).
- ³⁶P. D. Bogdanoff and B. Fultz, *Philos. Mag. B*, **79**, 753 (1999).
- ³⁷G. Garbulsky, Ph.D. Thesis, <http://africa.mit.edu/papers>.

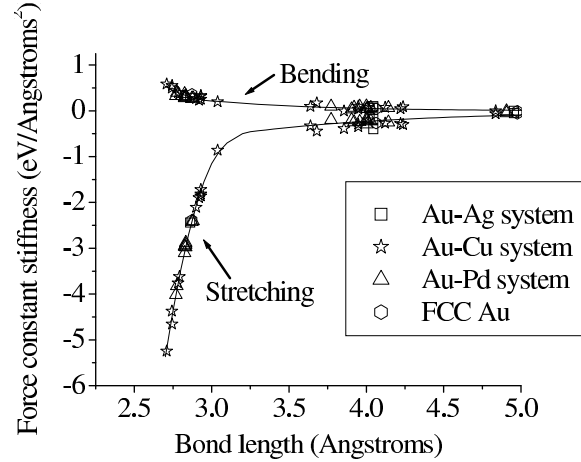


FIG. 1: Stiffness of bending and stretching force constants vs. bond length for Au-Au bonds. Force constants for the same system are represented by the same symbol (for example, all Au-Au bonds for $L1_2$ Au_3Cu use the same symbol). Lines are drawn as guides to the eye.

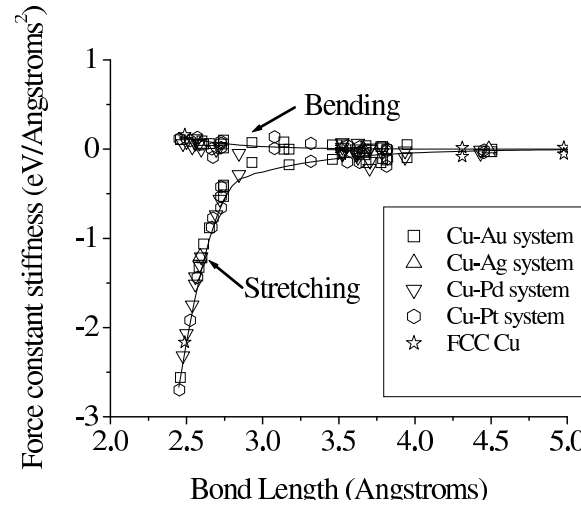


FIG. 2: Stiffness of bending and stretching force constants vs. bond length for Cu-Cu bonds. Lines are drawn as guides to the eye.

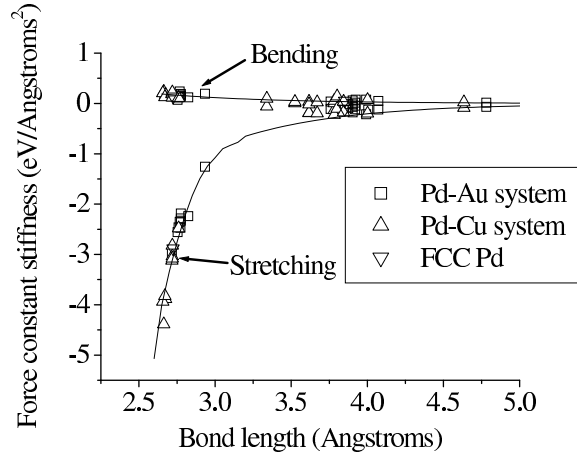


FIG. 3: Stiffness of bending and stretching force constants vs. bond length for Pd-Pd bonds. Lines are drawn as guides to the eye.

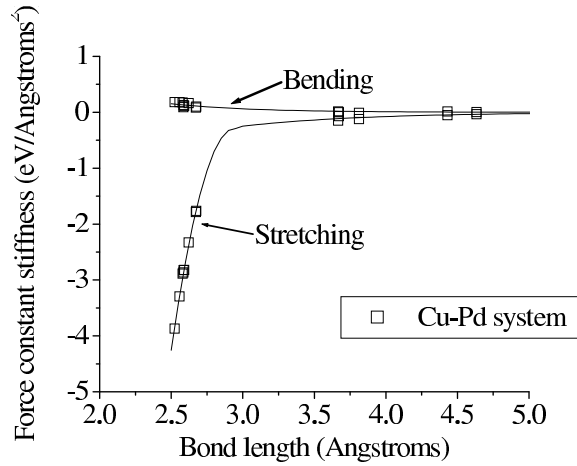


FIG. 4: Stiffness of bending and stretching force constants vs. bond length for Cu-Pd bonds. Lines are drawn as guides to the eye.

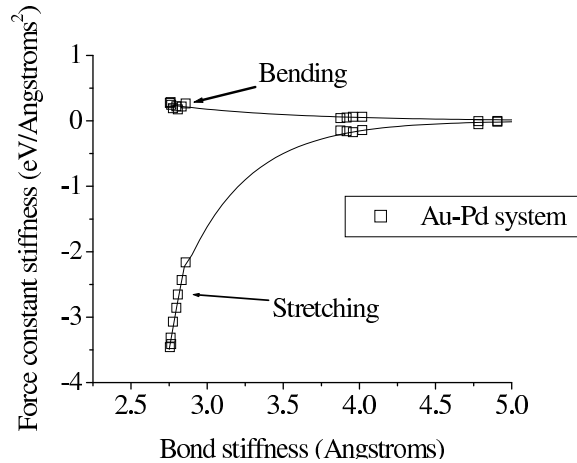


FIG. 5: Stiffness of bending and stretching force constants vs. bond length for Au-Pd bonds. Lines are drawn as guides to the eye.

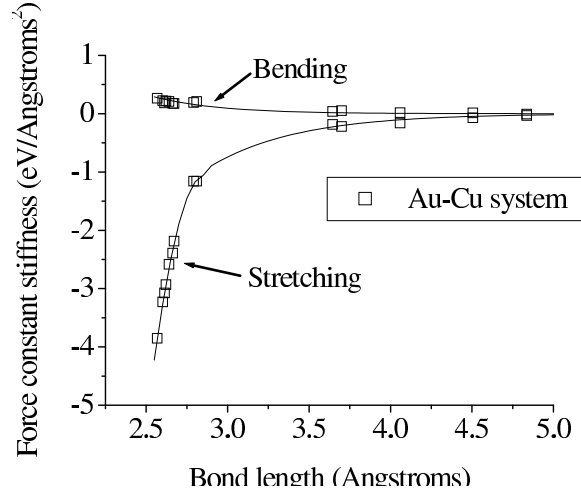


FIG. 6: Stiffness of bending and stretching force constants vs. bond length for Au-Cu bonds. Lines are drawn as guides to the eye.

Structure	Neighbors used in full force constant Calculation	$S_{vib}^{calc, all \, neigh, full \, fc}$	$S_{vib}^{calc, all \, neigh, sb}$	$S_{vib}^{calc, 1nn, full \, fc}$	$S_{vib}^{calc, 1nn, sb}$	$S_{vib}^{fit, 1nn, sb}$	$(S_{vib}^{calc, all \, neigh, full \, fc} - S_{vib}^{fit, 1nn, sb})$
Pd ₃ Cu L1 ₂	5	-4.56	-4.55	-4.59	-4.59	-4.57	+0.01
Pd ₃ Cu SQS8	2	-4.53	-4.53	-4.53	-4.53	-4.55	+0.02
Pd ₃ Au L1 ₂	3	-4.23	-4.23	-4.21	-4.21	-4.17	-0.06
Pd ₃ Au SQS8	2	-4.16	-4.16	-4.15	-4.15	-4.15	-0.01
Cu ₃ Pd L1 ₂	3	-4.73	-4.72	-4.70	-4.70	-4.76	-0.03
Cu ₃ Pd SQS8	2	-4.76	-4.76	-4.76	-4.76	-4.76	-0.00
Cu ₃ Au L1 ₂	3	-4.31	-4.30	-4.28	-4.27	-4.28	-0.03
Cu ₃ Au SQS8	2	4.24(0.03)	-4.24	-4.27	-4.27	-4.27	+0.04
Au ₃ Pd L1 ₂	5	-3.40	-3.40	-3.42	-3.41	-3.40	+0.00
Au ₃ Pd SQS8	2	-3.45	-3.45	-3.45	-3.45	-3.40	-0.05
Au ₃ Cu L1 ₂	5	-3.24	-3.21	-3.21	unstable	-	-
Au ₃ Cu SQS8	2	-3.25	unstable	-3.24	unstable	-	-
Cu ₃ Pt L1 ₂	3	-4.54	-4.53	-4.52	-4.51	-	-
Cu ₃ Pt SQS8	2	-4.52	-4.51	-4.51	-4.50	-	-
Ag ₃ Au L1 ₂	3	-3.57	-3.56	-3.55	-3.54	-	-
Au ₃ Ag L1 ₂	2	-3.17	-3.17	-3.13	-3.13	-	-

TABLE I: Vibrational entropy data. Listed are vibrational entropies calculated with all neighbors and full force constant matrices, vibrational entropies calculated with all neighbors and stretching-bending force constants, calculated vibrational entropy with first-nearest neighbors and full force constant matrices, calculated vibrational entropy with first-neighbors and stretching-bending force constant matrices, and fit-vibrational entropies using first-neighbors and stretching-bending force constants. Also listed is $(S_{vib}^{calc, all} - S_{vib}^{fit, 1nn})$, the error introduced by using fit force constants, the stretching-bending force constant model, and first-nearest neighbor force constants. Errors are $0.015 \, k_B$ unless otherwise indicated. All numbers are rounded to $0.01 \, k_B$.

Structure	Neighbors used in full force constant	S_{vib}	S_{vib}^{1nn}	$S_{vib}^{fit,1nn}$	$(S_{vib}^{calc,all} - S_{vib}^{fit,1nn})$
		Calculation	All neighbors, full force constants (k_B)	1nn, full force constants (k_B)	Fit stretching and bending terms, 1nn (k_B)
Pd ₃ Cu L1 ₂ (2%)	5	-4.41	-4.44	-4.42	0.01
Pd ₃ Cu L1 ₂ (4.5%)	5	-4.30	-4.33	-4.31	0.01
Pd ₃ Cu L1 ₂ (6.0%)	5	-4.14	-4.17	-4.16	0.02
Pd ₃ Cu SQS8 (2%)	2	-4.39	-4.37	-4.40	0.01
Pd ₃ Au L1 ₂ (2%)	3	-4.08	-4.06	-4.02	-0.05
Pd ₃ Au SQS8 (2%)	2	-4.01	-4.00	-3.99	-0.02
Cu ₃ Pd L1 ₂ (2%)	3	-4.61	-4.58	-4.64	+0.03
Cu ₃ Pd SQS8 (2%)	2	-4.63	-4.62	-4.62	-0.01
Cu ₃ Au L1 ₂ (2%)	3	-4.18	-4.15	-4.13	-0.05
Cu ₃ Au SQS8 (2%)	2	-4.12	-4.14	-4.13	+0.01
Au ₃ Pd L1 ₂ (2%)	5	-3.24	-3.26	-3.27	+0.03
Au ₃ Pd SQS8 (2%)	2	-3.28	-3.27	-3.23	-0.05

TABLE II: Vibrational entropies at increased volume. Percentage increase in volume is indicated in parenthesis. Listed are vibrational entropies calculated with all neighbors and full force constant matrices, vibrational entropies calculated with fit first-nearest neighbor stretching-bending force constants, and $(S_{vib}^{calc,all\,neigh,\,full\,fc} - S_{vib}^{fit,1nn,\,sb})$. All numbers are rounded to 0.01 k_B .

System	$\Delta S_{vib}^{calc, all \text{ neighbors}, full \text{ fc}}$	$\Delta S_{vib}^{fit, 1nn, sb}$	$\Delta S_{vib}^{calc, all \text{ neighbors}, full \text{ fc}} - \Delta S_{vib}^{fit, 1nn, sb}$
	All neighbors, full force constants (k_B)	Fit stretching and bending terms, 1nn (k_B)	
Pd ₃ Cu SQS8 – Pd ₃ Cu L1 ₂	+0.03	+0.05	+0.02
Pd ₃ Au SQS8 – Pd ₃ Au L1 ₂	+0.07	+0.02	+0.05
Cu ₃ Pd SQS8 – Cu ₃ Pd L1 ₂	+0.03	+0.00	+0.03
Cu ₃ Au SQS8 – Cu ₃ Au L1 ₂	+0.07	+0.00	-0.06
Au ₃ Pd SQS8 – Au ₃ Pd L1 ₂	-0.05	-0.04	+0.01
Pd ₃ Cu L1 ₂ (2%) – Pd ₃ Cu L1 ₂	+0.14	+0.15	+0.00
Pd ₃ Cu SQS8 (2%) – Pd ₃ Cu SQS8	+0.14	+0.15	-0.01
Pd ₃ Au L1 ₂ (2%) – Pd ₃ Au L1 ₂	+0.15	+0.15	+0.01
Pd ₃ Au SQS8 (2%) – Pd ₃ Au SQS8	+0.15	+0.16	-0.02
Cu ₃ Pd L1 ₂ (2%) – Cu ₃ Pd L1 ₂	+0.12	+0.12	+0.00
Cu ₃ Pd SQS8 (2%) – Cu ₃ Pd SQS8	+0.13	+0.14	-0.01
Cu ₃ Au L1 ₂ (2%) – Cu ₃ Au L1 ₂	+0.12	+0.15	-0.02
Cu ₃ Au SQS8 (2%) – Cu ₃ Au SQS8	+0.12	+0.14	-0.02
Au ₃ Pd L1 ₂ (2%) – Au ₃ Pd L1 ₂	+0.16	+0.13	-0.03
Au ₃ Pd SQS8 (2%) – Au ₃ Pd SQS8	+0.17	+0.17	+0.00
Pd ₃ Cu L1 ₂ (4.5%) – Pd ₃ Cu L1 ₂	+0.25	+0.26	+0.00
Pd ₃ Cu L1 ₂ (6.0%) – Pd ₃ Cu L1 ₂	+0.42	+0.41	+0.00

TABLE III: Vibrational entropy differences. Listed are vibrational entropy differences upon disordering and vibrational entropy differences between the same structure at different volumes. Percentage increase in volume is indicated in parenthesis. Also shown are errors in differences, $\Delta S_{vib}^{calc, all \text{ neighbors}} - \Delta S_{vib}^{fit, 1nn}$.